NUMERICAL STUDY OF TURBULENT WAKES IN BACKGROUND TURBULENCE

John A. Redford and Gary N. Coleman
School of Engineering Sciences, University of Southampton,
Highfield, Southampton, SO17 1BJ, UK.
j.a.redford@soton.ac.uk and g.n.coleman@soton.ac.uk

ABSTRACT

Time-developing axisymmetric turbulent wakes with background turbulence are studied through Direct Numerical Simulation (DNS). A velocity field from turbulent wake and isotropic turbulence simulations have been fused together to produce the initial condition. Cases for which the background turbulence has a greater length scale than the wake are considered. Visualizations of the results are included along with plots showing how quickly the wake merges with the background. The turbulent background has a profound effect on the wake, which is not surprising, but the results here can help to quantify the effects. For example the stronger background has a greater effect on the wake, causing a reduction in the time taken for the wake and background to merge. Also, the effects of the background turbulence on some wake statistics only emerge after some time.

INTRODUCTION

Most turbulent wake experiments have been done in a wind tunnel or water channel where the background turbulence is minimized (e.g. Uberoi & Freymuth, 1970). No study of wakes with background turbulence seems to exist[1], despite the fact that in most real situations wakes are created in flows with preexisting disturbances. Two examples that spring to mind are wakes within the ocean mixed layer or in a turbomachinery environment.

In a study of wakes with background turbulence practical difficulties arise due to the large number of relevant parameters. In addition to the normal parameters (such as Reynolds number) that define the individual wake and isotropic turbulence flows, the turbulent wake and the background have different turbulence kinetic energy and length scales relative to each other. Further complications arise due to the time dependence associated with the decay of the turbulence in both constituent flows. This makes it challenging to formulate a 'clean' test. Assuming the energy level and length scale of the wake can be greater, equivalent and less than that of the background there are nine different combinations to consider.

In this paper the method by which precursor simulations of the turbulent wake and background are fused together is explained. Briefly, combining the wake and background fields involves surrounding the instantaneous velocity distribution from the wake with that from the decaying isotropic turbulence – which amounts to removing a 'wrinkled core' from the latter, and filling the resulting void with the instantaneous wake velocity field. The combined field is then used as the turbulent initial condition for the wake/background DNS, for which results are shown below.

[1]See for example Prof. Bradshaw's bibliography, http://navier.stanford.edu/bradshaw/pbref/pbref.html

METHOD

Equations of motion and numerics

We make use of the incompressible Navier-Stokes equations. In non-dimensional form these are

$$\frac{\partial U_i}{\partial x_i} = 0 \qquad (1)$$

$$\frac{\partial U_i}{\partial t} = \epsilon_{ijk} u_j \omega_k - \frac{\partial \tilde{p}}{\partial x_i} - \frac{1}{\mathrm{Re}_{\mathrm{ref}}} \frac{\partial^2 U_i}{\partial x_j \partial x_j} + F, \qquad (2)$$

where $x_i = x_i^*/L_{\mathrm{ref}}^*$ is the Cartesian coordinate system, $t = t^* U_{\mathrm{ref}}^*/L_{\mathrm{ref}}^*$ is time, $U_i = U_i^*/U_{\mathrm{ref}}^*$ is velocity, $\omega_i = \epsilon_{ijk}\partial U_k/\partial x_j$ is vorticity, $\tilde{p} = p_*'/\rho^* U_{\mathrm{ref}}^{*2} + \frac{1}{2}U_j U_j$ is pressure, $F = F^*/\rho^* U_{\mathrm{ref}}^{*2}$ is a body force, ρ^* is the fluid mass density, ν^* is the kinematic viscosity, ϵ_{ijk} is the permutation symbol, and an asterisk indicates a dimensional quantity. The nondimensional reference Reynolds number, $\mathrm{Re}_{\mathrm{ref}} = U_{\mathrm{ref}}^* L_{\mathrm{ref}}^*/\nu^*$, is written in terms of the reference velocity and length scale, U_{ref}^* and L_{ref}^* respectively.

Due to Galilean invariance, we need only be concerned with the velocity deficit (Tennekes & Lumley, 1972). The reference velocity is thus defined as the maximum axial mean velocity deficit $U_{\max}^* = \overline{U}_{\max}^*$, where the overbar denotes an average in the axial x_1 and the azimuthal directions. The wake half-width $\ell_{1/2}^*$ is twice the distance from the wake centreline (the mean wake centreline is assumed not to deviate through the wake simulation) to the point at which the axial mean velocity is half $U_{\max}^*$. The local time dependent wake Reynolds number is defined as $\mathrm{Re}_\ell(t) = U_{\max}^*(t)\ell_{1/2}^*(t)/\nu^* = \mathrm{Re}_{\mathrm{ref}} U_{\max}\ell_{1/2}$, where $U_{\max} = \overline{U}_{\max}^*/U_{\mathrm{ref}}^*$ and $\ell_{1/2} = \ell_{1/2}^*/L_{\mathrm{ref}}^*$. Here we choose for reference quantities the maximum wake velocity deficit and the wake half-width at the time t_0^* when the turbulent background is introduced as the reference quantities, i.e. $U_{\mathrm{ref}}^* = U_{\max}^*(t_0^*)$ and $L_{\mathrm{ref}}^* = \ell_{1/2}^*(t_0^*)$, such that $\mathrm{Re}_{\mathrm{ref}} = \mathrm{Re}_\ell(t_0)$. At other times the wake Reynolds number is $\mathrm{Re}_\ell(t) = \mathrm{Re}_{\mathrm{ref}} U_{\max}(t)\ell_{1/2}(t)$.

Solutions of (1) and (2) are found using the pseudo-spectral method with discrete Fourier transforms in each spatial direction and 3/2 de-aliasing. Time integration of the viscous terms is carried out by an integration factor (Rogallo, 1981) and for all other terms a third-order Runge-Kutta scheme is used (Spalart *et al.*, 1991). The wake with background simulations in both cases have a grid where the dimensions of the domain are $100\pi L_{\mathrm{ref}}^* \times 12.5\pi L_{\mathrm{ref}}^* \times 12.5\pi L_{\mathrm{ref}}^*$ and the number of Fourier modes is $3072 \times 288 \times 288$ in the x_1, x_2 and x_3 directions, respectively. Each time step took just over an hour of computer time (split over 48 processors on the UK HPCx system) and there are 1000 to 1200 time steps in each run.

Turbulence statistics

The wake is surrounded by the turbulent background, so provided the total size of the domain is large enough, after some time the wake turbulence will eventually become indistinguishable from the background. We are interested in the rate at which the merging happens, and it is expected that the wake-to-background ratios of turbulence kinetic energy and length scale will be important parameters. The changes in structure of the turbulence within the wake will also be interesting. The statistics are gathered at $r = \ell_{1/2}/2$ (where r is the distance from the mean wake centreline) because this is the point of maximum shear, and at the edge of the domain (in the background). Averaging is in the x_1 and azimuthal directions where the flow is homogeneous.

The characteristic velocity of the turbulence is chosen to be the root-mean-square of the velocity fluctuation

$$u_i' = \sqrt{\overline{u_i u_i}}, \tag{3}$$

where u_i is the perturbation from the mean velocity ($U_i = \overline{U}_i + u_i$). Also of use is the mean turbulent kinetic energy $k = \frac{1}{2}\overline{u_i u_i}$. The longitudinal Taylor microscale is calculated as

$$\lambda_f = 2u_1'^2 \Bigg/ \overline{\left(\frac{\partial u_1}{\partial x_1}\right)^2}. \tag{4}$$

By combining the velocity and length scale a turbulence Reynolds number can be defined as $\mathrm{Re}_\lambda = u_1'^* \lambda_f^* / \nu^*$.

The structure functions indicate differences in the internal state of turbulence. The mean shear imposed by the wake causes the turbulence in the wake and background to have different values of the structure function. The third order structure function (or velocity derivative skewness) is defined as

$$\gamma = \overline{\left(\frac{\partial u_1}{\partial x_1}\right)^3} \Bigg/ \left[\overline{\left(\frac{\partial u_1}{\partial x_1}\right)^2}\right]^{3/2}. \tag{5}$$

For fully developed turbulence the velocity derivative skewness should be negative and constant.

The wake and background will have a different spectral energy distribution. For purposes of comparison we use the one-dimensional energy spectrum

$$E_{11} = \widehat{u}_i(\kappa_1)\widehat{u}_i(\kappa_1)^{\#}, \tag{6}$$

where hat $(\widehat{\ldots})$ denotes Fourier coefficient, superscript $\#$ denotes a complex conjugate, and κ_i is the wavenumber.

As the wake turbulence is strained by the mean flow, anisotropy will be introduced into the turbulence. To quantify the anisotropy we use a single component of the anisotropy tensor

$$b_{xr} = \frac{\overline{u_1 u_r}}{\overline{u_i u_i}}, \tag{7}$$

where the r subscript indicates a vector pointing in the radial direction.

INITIAL CONDITION

In nature or experiment the most likely situation is that the wake is produced with the background turbulence already in existence. Also, it is often the case that the kinetic energy within the wake is initially far greater than the background. Computationally a wake could be created within the background using a body force, and this was attempted, but the constraints of the simulation mean that the wake and background have to be similar in velocity and length scale. As a result the wake is heavily distorted before it becomes turbulent.

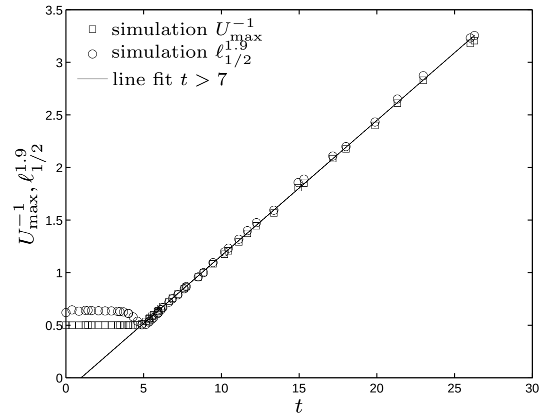

Figure 1: Development of the turbulent wake with self-similar scaling.

A simpler, but less physical approach, is to take isotropic turbulence and a fully developed turbulent wake and superimpose them together. The hope is that any non-physicality will quickly disappear and then the wake will behave like it would in the real situation. Initially the superposition was just a simple addition of the velocity fields but improvement was made by cutting a core out of the background turbulence so that the wake could be added without disturbing the structure of the wake turbulence.

Turbulent wake

A time-developing wake has to be prescribed with perturbations that will grow into turbulence, and the closer the wake initial condition is to physical fluid motion the shorter the time taken to realize turbulence. With this in mind the turbulent wake has been initialized using a series of laminar vortex rings (Redford *et al.*, 2007). After some time the vortex rings break down and merge together to form a turbulent wake. The wake initialized with vortex rings is advantageous compared with the more conventional approach, where the perturbation is random noise, because the time taken for the turbulence to become fully developed is shorter and the Reynolds number at this point is higher.

An important property exhibited by fully developed turbulent wakes is self similarity (Tennekes & Lumley, 1972). Self similarity of a turbulent shear flow stipulates that the mean velocity profile at every station (or in this case time) is the same when normalized by an appropriate velocity and length scale, e.g. $U_{\max}$ and $\ell_{1/2}$. A consequence of the uniqueness of the collapse of velocity profiles is that the development of $U_{\max}$ and $\ell_{1/2}$ should satisfy a power law relationship in time. For the current wake simulation the collapse of data (Figure 1) shows $U_{\max} \propto t^{-1}$ and $\ell_2 \propto t^{1/1.9}$. Traditionally the axisymmetric turbulent wake has been thought to developed according to $U_{\max} \propto t^{-2/3}$ and $\ell_{1/2} \propto t^{1/3}$ (Tennekes & Lumley, 1972). However, some doubt has been cast on this as a general rule applicable to all axisymmetric wakes (Pope, 2000) – doubt that is reinforced by the current results (see Figure 1).

To initialize the wake simulation with background turbulence we need to choose from the times shown in Figure 1. Our choice is motivated by two opposing factors. First, the wake should be fully developed, because earlier tests have shown a wake with early turbulent structures struggles to survive in the turbulent background. Second, the wake should have a sufficient Reynolds number, so that there are

Table 1: Turbulence parameters at the wake half width of the wake when the background is introduced.

u_1'	λ_f	Re_λ	γ
0.20	0.14	106	-0.42

a range of scales of turbulent motion within the wake. The difficulty with an axisymmetric wake is that the Reynolds number is decaying so it is necessary to take the sample as early as possible. Taking these factors into consideration the wake at $t_0 = 9$ is chosen, because there has already been a period of self-similar growth and the wake Reynolds number is 3800, which is reasonable based on past experience.

Table 1 shows some turbulence statistics at the wake half-width when the background turbulence is introduced. It will be important later on to compare the wake turbulence with that of the background, as along with the wake velocity and half-width, they are expected to govern the interaction.

Generation of background turbulence

In creating the background turbulence there are several requirements. First, the energy spectrum should have a distinct energy containing range, inertial range and dissipation range that prevents a buildup of energy at high wavenumbers. This is achieved when the domain is large in comparison with the turbulent length scales and the Reynolds number is high, but computational resources limit this. Second, the anisotropy of the turbulence must be well defined. We start with simplest scenario of isotropic turbulence. Once these two are achieved the intensity and length-scale of the background turbulence can be varied to create a variety of initial conditions.

Isotropic background turbulence is created using a similar method to that of Kerr (1985, 1990), Bogucki *et al.* (1997) and Gotoh *et al.* (2002). The DNS includes a forcing term (F in equation (2)) that maintains the energy of the low wavenumber Fourier modes in a sphere of radius $2.5\Delta|\boldsymbol{\kappa}|$ centred at $|\boldsymbol{\kappa}| = 0$ after each time step. The forcing is applied to the Fourier transformed velocity field by multiplying each component within the sphere by the same factor.

The initial flow field consists of Gaussian random numbers scaled by $\widehat{u} = C\exp(-ck)$, where $C = 10^{-1}$ and $c = 10^{-2}$ are arbitrary, because the turbulence properties can be changed later with adjustment of the reference Reynolds number or forcing. As the simulation steps through time, the flow field is arranged into coherent turbulence. In the interest of efficiency, we use the method of Bogucki *et al.* (1997) and Gotoh *et al.* (2002), that starts with a coarse grid at low Reynolds number, then resolution and Reynolds number are increased in subsequent runs. When the simulation is restarted with different properties, some time is required before the changes permeate throughout the spectrum.

The background turbulence is initially developed in a cubic domain but to be compatible with the wake, the domain size has to be greater in the axial direction. The streamwise expansion is carried out with Fourier methods, exploiting the flow periodicity. The Fourier modes are given extra energy in the form of Gaussian random noise which will break the symmetry within the flow. The background turbulence is then run for more time until the spectrum becomes steady once again.

The turbulence that was achieved at the end of this process was too strong for the intended wake so more time-stepping was used without low frequency forcing to allow the turbulence to decay to the desired level. After the two flows are combined (see next section) the background turbulence will be free to decay so it is probably advantageous if there is some free decay beforehand. Two fields of background turbulence have been generated in this way, one with a greater turbulent kinetic energy (stronger turbulence) and one that has decayed to a state of lower turbulent kinetic energy (weaker background turbulence).

Table 2: Properties of the turbulent background.

background	u_1'	λ_f	Re_λ	γ
Weaker	0.13	0.32	160	-0.54
Stronger	0.25	0.25	232	-0.5

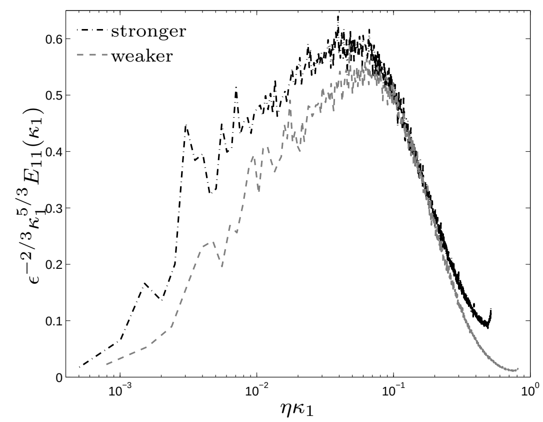

Figure 2: Background turbulence spectra.

Some details of the two turbulent backgrounds used here are given in Table 2. The weaker background, having decayed for more time than the stronger, has a lower velocity fluctuation by approximately half and the length scale has increased by about 30%. The second-order structure function γ is approximately -0.5 in both cases, which is the value that is often found in other numerical simulations of isotropic turbulence (Bogucki *et al.*, 1997; Gotoh *et al.*, 2002).

In Figure 2 a scaling is used to show how much inertial range ($\kappa^{-5/3}$) the simulated turbulence has. In the case of the stronger background turbulence there is a short but distinct $\kappa^{-5/3}$ range, but for the weaker background it is shorter still and difficult to pick out. It is important that some inertial range is achieved so that the turbulence is representative of practical engineering and geophysical applications, but there are a number of factors that prevent this. For example, the finite computational resources, and also the need to accommodate the wake turbulence, which has a different length scale to the background turbulence. We hope to address this shortcoming in future simulations.

The wavenumbers of the spectra shown in Figure 2 are normalized with the local Kolmogorov length scale

$$\eta^* = \left(\nu_*^3/\epsilon^*\right)^{1/4}, \tag{8}$$

where $\epsilon^* = 2\nu^*\overline{s_{ij}^* s_{ij}^*}$ is the rate of dissipation of turbulent kinetic energy, and the fluctuating rate of strain is

$$s_{ij} = \frac{1}{2}\left(\frac{\partial u_i}{\partial x_j} + \frac{\partial u_j}{\partial x_i}\right). \tag{9}$$

The weaker background comes close to the Kolmogorov

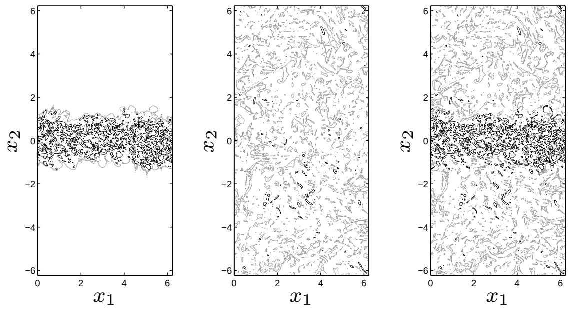

(a) (b) (c)

Figure 3: Contours of vorticity magnitude $|\boldsymbol{\omega}| = 0.002, 0.02$ (grey, black respectively), (a) the wake (b) the weaker background and (c) the wake and background combined.

length scale and consequently there is no detectable energy buildup at the top of the spectrum. The stronger background turbulence has a slight buildup of energy. However, in the wake simulations the number of modes is increased by a factor of 1.5 in the streamwise direction and by 9/8 in the spanwise direction to $3072 \times 288 \times 288$, which also improves the resolution of the background turbulence.

Application of the Kolmogorov hypothesis shows that the one-dimensional energy spectrum within the inertial subrange (Pope, 2000) should be given by $E_{11} = C_1 \epsilon^{2/3} \kappa_1^{-5/3}$, where $C_1 = 0.49$. The limited inertial range in Figure 2 is close to the theory.

Combining the wake and background

After the wake and background have developed independently, it is necessary to find a rational process by which they can be combined. The most important objective is to preserve the flow structure within the wake and to a lesser extent the background. To ensure the wake is not contaminated with the background flow, a 'cut' is made from the background before the two flows are combined. The cut amounts to removing a 'wrinkled core' from the background turbulence. The threshold at which the background is cut is decided using the instantaneous velocity magnitude of the $t = t_0$ realization of the wake simulation. When the velocity magnitude in the wake simulation is greater than 5% of the maximum the wake velocity is used, otherwise the background turbulence is used. Figure 3 shows that the respective structure of the wake and background flows has been maintained. Some additional weak spurious structures have appeared at the interface between the wake and background, so it is necessary to assume that some time will be required for the turbulence in this region to recover.

The turbulence spectrum contains information on the length scales and kinetic energy of the turbulence. The scaling of Figure 4 means that the $\kappa = 0$ intercept with the vertical axis defines an integral length scale with

$$L_{11} = \frac{\pi E_{11}(0)}{2\overline{u_1^2}}. \tag{10}$$

Figure 4 implies that the length-scale of the background turbulence is an order of magnitude greater than the wake turbulence.

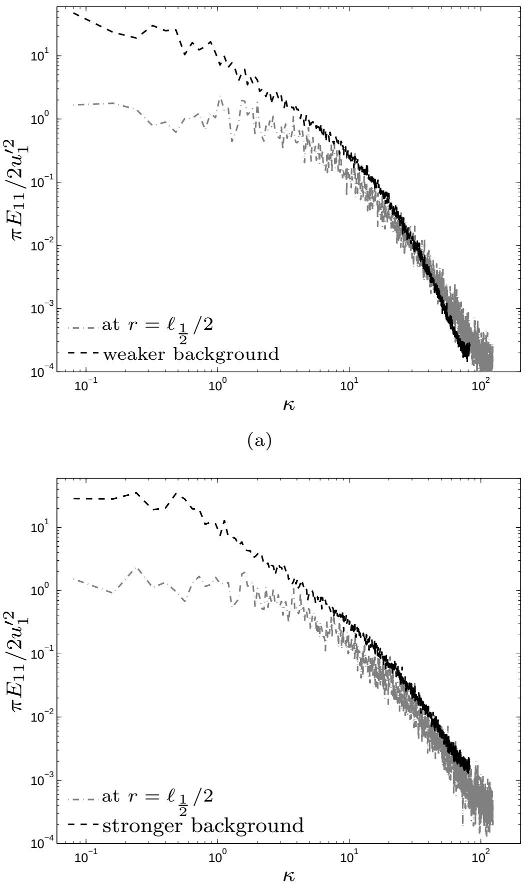

(b)

Figure 4: The initial energy spectra at the wake half width and in the background. (a) Weaker background turbulence and (b) stronger background turbulence.

RESULTS

Flow visualization

The result of the superposition of vorticity is shown in Figure 5(a). A low contour level of vorticity is used to highlight the background turbulence while a contour level an order of magnitude greater allows the wake to be seen. The method used appears to have been successful, as there is a sharp change in the contour levels from grey to black at the edge of the wake.

After the simulation has run for some time the background begins to make incursions into the wake. In some places the higher vorticity wake turbulence has been completely replaced by the lower vorticity that will have mostly come from the background. The processes by which the wake is 'washed away' more in some regions than others shows that local events and interactions between the wake and background matter. The wake will become less visible after the time shown in Figure 5(b), but it will be interesting to see which if any turbulence statistics continue to contain the characteristics of the wake.

Development of a wake with turbulent background

Shortly after the turbulent wake and background are combined the decay of the velocity deficit increases (Fig-

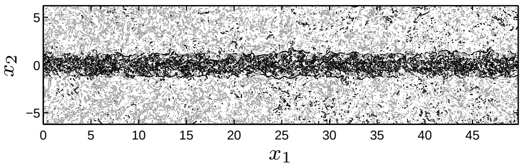

(a)

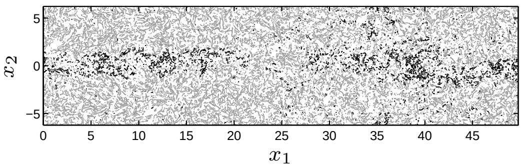

(b)

Figure 5: The wake with weaker background turbulence. Contours of vorticity $|\boldsymbol{\omega}| = 0.002, 0.02$ (grey, black respectively) at t (a) 8.9 when the background is introduced and c) 14.5. A slice is taken through the domain along the wake centreline.

ure 6(a)). However, Figure 6(b) shows no immediate effect of background turbulence on the wake half width. Instead after some time the wake starts to spread more quickly. It is not immediately obvious why a property along the wake centre should be affected more than another property at the half width. Figure 6(c) shows the wake velocity profile at $t = 13$, where the velocity deficit at the wake centre has decreased by 20% more with the weaker background turbulence, but the wake half width has increased by only 8%. The reason for this is found in Figure 6(c). At $t = 13$, the background turbulence has been entrained into the edges of the wake, causing the additional spreading in this region but the direct effect at the wake half width is negligible. To maintain constant net momentum the velocity at the centre of the wake is reduced to compensate.

Increasing the kinetic energy of the background turbulence causes a greater decay in velocity deficit and the time period before the wake width is affected, is shortened by about a quarter. So as well as the background turbulence having a greater effect on the wake it is also entrained quicker.

Effect on wake turbulence

After the wake and background are combined, the turbulence kinetic energy within the wake rises (Figure 7(a)). The rise is even observed when the background turbulence has less turbulent kinetic energy than the wake. In the case where background turbulent kinetic energy is stronger, the wake turbulence increases in kinetic energy until it is the same as the background.

From Figure 7(a) it is evident that two very different wake-background kinetic energy ratios have been achieved. The effect of a large variation in length scale ratio on the wake development is yet to be explored, since at this point there is only a small variation of the background turbulence λ_f available (Table 2). This will be considered in future simulations.

Figure 7(b) shows that the anisotropy of the turbulence within the wake is greater than the background. It was intended that each realization of background turbulence would be isotropic, but presumably due to the finite size of the domain, this is difficult to achieve exactly. However, there is a clear separation between wake and background turbulence. When the weaker background turbulence is introduced there is a slow change toward the background, but with the stronger background, the turbulence within the wake very quickly tends toward the isotropic background state. The anisotropy of the turbulence is generated by the straining of turbulence by the mean flow, so when the background turbulence is stronger not only is the wake infiltrated by the background turbulence, but the wake is distorted so much that none of its structure remains.

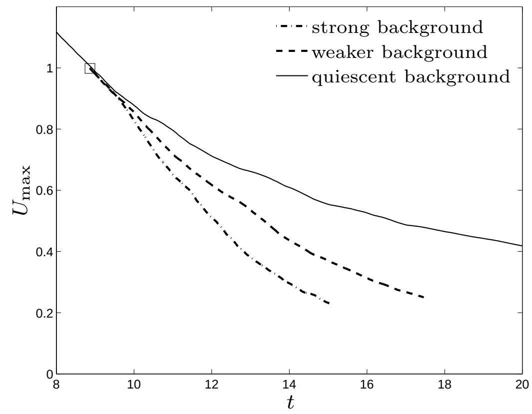

(a)

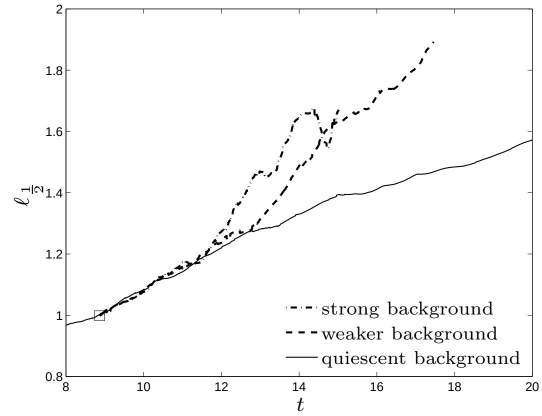

(b)

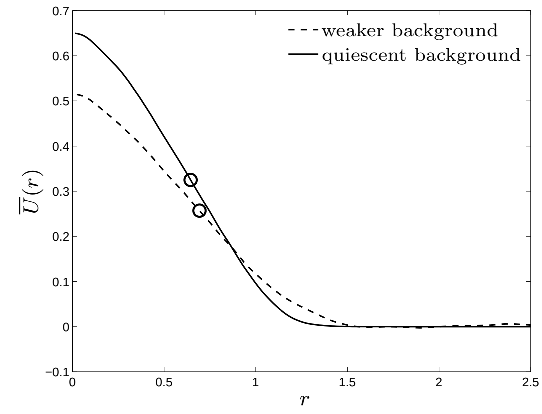

(c)

Figure 6: Mean flow parameters. Wake velocity deficit (a) and width (b); the point at which background turbulence is introduced is marked with a square. Velocity profiles at $t = 13$ (c); the circles mark the wake half width.

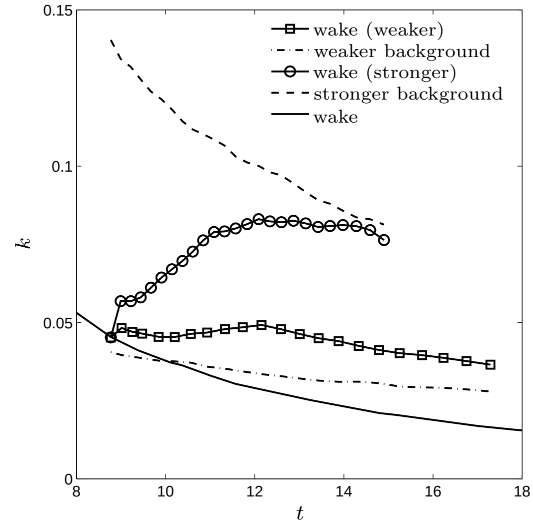

(a)

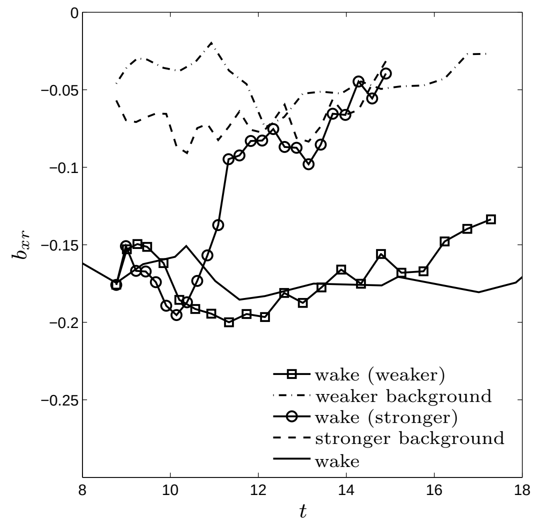

(b)

Figure 7: Turbulence statistics at the wake half width and in the background, (a) turbulent kinetic energy (b) streamwise-radial anisotropy tensor.

DISCUSSION

The turbulent background clearly has a great effect on the turbulent wake. The reduction in the wake local Reynolds number is accelerated by the introduction of background turbulence. Decay of the wake is increased because the incursions of the background turbulence into the wake have the effect of breaking it up in some places. The additional input of turbulent kinetic energy from the background means that the reduction of the turbulence level at the same rate as the velocity deficit is no longer possible. Instead there is an unusually high level of turbulence in the wake and the mean flow develops more rapidly. As the background turbulence makes incursions into the wake the turbulence statistics of the wake and background merge, particularly when the background turbulence has a greater turbulent kinetic energy.

SUMMARY

A wake with background turbulence has been simulated, for cases where the wake turbulence has a smaller length scale. Visualizations show that the wake is broken up by the background turbulence. The background turbulence causes the decay in velocity deficit to increase and after a time delay the wake width to increase at a greater rate. The turbulence statistics in the wake tend toward the background levels.

Much more of the parameter space should be explored. To do this the range of background turbulence length scales need to be increased. Possibly some changes to the low frequency forcing when developing the background turbulence could help.

ACKNOWLEDGMENT

This work was supported by extra-mural funding from the UK Ministry of Defence (Dstl contract RD027-02854). The simulations were run on the UK EPSRC HPCx IBM supercomputer, and the computer time was provided by the UK Turbulence Consortium. We thank Mr. P.J. Archer, Prof. I.P. Castro, Dr. R.P. Hornby, Dr. T.G. Thomas, Dr. S.N. Yakovenko, and Dr. C.P. Yorke for the invaluable discussions.

REFERENCES

Bogucki, D., Domaradzki, J. and Yeung, P., 1997, "Direct numerical simulations of passive scalars with Pr > 1 advected by turbulent flow.", *J. Fluid Mech.*, Vol. 343, pp. 111–130.

Gotoh, T., Fukayama, D. and Nakano, T., 2002, "Velocity field statistics in homogeneous steady turbulence obtained using a high-resolution direct numerical simulation.", *Phys. Fluids*, Vol. 14 (3), pp. 1065–1081.

Kerr, R., 1985, "Higher-order derivative correlations and the alignment of small-scale structures in isotropic numerical turbulence." *J. Fluid Mech.*, Vol. 153, pp. 31–58.

Kerr, R., 1990, "Velocity, scalar and transfer spectra in numerical turbulence." *J. Fluid Mech.*, Vol. 211, pp. 309–332.

Pope, S., 2000, *Turbulent Flows*, Cambridge University Press.

Redford, J., Yorke, C. and Coleman, G., 2007, "The effect of initial conditions on a time developing turbulent wake." *In preparation.*

Rogallo, R., 1981, "Numerical experiments in homogeneous turbulence.', NASA Technical Memorandum 81315.

Spalart, P., Moser, R. and Rogers, M., 1991, "Spectral methods for the Navier–Stokes equations with one infinite and two periodic directions.", *J. Comput. Phys.*, Vol. 96 (2), pp. 297–324.

Tennekes, H. and Lumley, J., 1972, *A first course in turbulence*, The MIT Press.

Uberoi, M. and Freymuth, P., 1970, "Turbulent energy balance and spectra of the axisymmetric wake.", *Phys. Fluids*, Vol. 13 (9), pp. 2205–2210.